

# Theoretical study of the migration of the hydrogen atom adsorbed on aluminum nanowire

Akinori Fukushima<sup>a</sup>, Kosuke Hirai<sup>a</sup>, Masato Senami<sup>a</sup>, Akitomo Tachibana<sup>a,\*</sup>

<sup>a</sup>*Department of Micro Engineering, Kyoto University, Kyoto 606-8501, Japan*

---

## Abstract

We study the behavior of a hydrogen atom adsorbed on aluminum nanowire based on density functional theory. In this study, we focus on the electronic structure, potential energy surface (PES), and quantum mechanical effects on hydrogen and deuterium atoms. The activation energy of the diffusion of a hydrogen atom to the axis direction is derived as 0.19 eV from PES calculations. The probability density, which is calculated by including quantum effects, is localized on an aluminum top site in both cases of hydrogen and deuterium atoms of the ground state. In addition, some excited states are distributed between aluminum atoms on the surface of the nanowire. The energy difference between the ground state and these excited states are below 0.1 eV, which is much smaller than the activation energy of PES calculations. Thus using these excited states, hydrogen and deuterium atoms may move to the axial direction easily. We also discuss the electronic structure of the nanowire surface using quantum energy density defined by one of the authors.

*Keywords:* quantum energy density, aluminum nanowire, behavior of a hydrogen atom, zero-point vibrational energy

---

## 1. Introduction

Recently, the development of experimental methods allows us to fabricate nanostructures experimentally. In these nanostructures, nanowire and nanotube, which have periodicity along one dimension, have remarkable characters compared with bulk system. In particular, nanowires are fabricated for various species of atoms, and hence it attracts much attention theoretically and industrially [1–15]. Nanowire has high ratio of surface area to its mass and therefore it is considered that nanowire structures are good candidates for hydrogen storage material which is a key ingredient for hydrogen energy system. Among various species of metal atoms, the aluminum atom exists abundantly on the earth and is available easily. Hydrogen storage material should have higher weight percent

---

\*Corresponding author, telephone and fax : +81-75-753-5184  
*Email address:* akitomo@scl.kyoto-u.ac.jp (Akitomo Tachibana)

storage ability so that hydrogen energy is comparable with fossil fuel. The aluminum atom has also smaller mass than those of most metal atoms. Therefore aluminum nanowire is a promising material for hydrogen storage.

From this viewpoint, we study aluminum nanowire in this work following previous works in our laboratory. Makita et al. showed stable geometries of aluminum nanowires based on Au nanowire [5]. Kawakami et al. showed that a hydrogen molecule is adsorbed on a pentagonal aluminum nanowire model as two separate hydrogen atoms [8]. Nakano et al. suggested to wrap aluminum species in carbon materials such as carbon nanotube to enhance the hydrogen adsorption on their surfaces [11]. In addition, geometry and hydrogen adsorption energy for AlB nanowire whose structure was based on aluminum nanowire was reported [15]. The aluminum nanowire with pentagonal ring is studied in this work following these works, since this structure is stable and has high ratio of surface area to the density.

A hydrogen atom is stabilized by about -3.6 eV after the adsorption on the nanowire [15]. Hence, it is not easy task to detach the adsorbed hydrogen atom from the nanowire. The hydrogen atom has high barrier for the direction perpendicular to the nanowire and the motion to the direction is not unlikely, and nevertheless hydrogen atoms may move along the nanowire. Therefore, in this work, we focus on the dynamics of hydrogen and deuterium atoms adsorbed on the aluminum nanowire. We calculate potential energy surface (PES) of a hydrogen atom adsorbed on the pentagonal aluminum nanowire. Using this result, we discuss the behavior of a hydrogen atom on the nanowire. Particularly, we compare the activation energies of the hydrogen move toward angular and axial directions. In addition, we focus on quantum effects of a hydrogen atom. We also study those of a deuterium atom for comparison. Since their masses are small, quantum effects, such as large zero-point vibrational energy and non-localization, are important for these atoms [13, 16, 17]. These phenomena affect the adsorption and activation energy of hydrogen and deuterium atoms. We calculate the wave functions of hydrogen and deuterium atoms with our PES. We also perform quantum energy density analysis, which is proposed by one of the authors, to discuss the surface of aluminum nanowire from a new physical viewpoint [18].

## 2. Computational Details

Total energy and electronic structure calculations are carried out based on density functional theory (DFT) with the projector augmented wave method by the Vienna ab initio simulation package [19, 20]. Electron wave functions are expanded by plane wave basis sets and the kinetic energy cut off is set to 250 eV. The exchange-correlation functional we used in this calculation is the generalized gradient approximation of Perdew, Burke, and Ernzerhof [21]. All calculations are carried out in the spin-polarized condition.

We show an aluminum nanowire model used in this study in fig. 1. The radius of nanowire ( $R$ ) and the distance between an aluminum pentagonal ring and an aluminum atom on the axis ( $D$ ) are derived as 2.47 Å and 1.23 Å,

respectively, from the optimization calculation. The differences from those of our previous papers are arisen from the difference of program code [1, 15]. The boundary condition of this nanowire model is imposed as periodic one. In our calculation,  $15.0 \text{ \AA} \times 15.0 \text{ \AA} \times 8D \text{ \AA}$  super cell is taken for all electronic structure calculations. This cell has a large enough vacuum region so that the interaction with next cells is negligible. The number of aluminum atoms in the unit cell is counted as twenty-four. A  $1 \times 1 \times 4$  k-point set is used to sample the Brillouin zone. For the density of state (DOS) calculations, a  $1 \times 1 \times 51$  k-point set is adopted.

This model has pentagonal rings whose angles are different by  $\pi/5$  from each other. For the PES calculation, the position of the hydrogen atom is parametrized in a cylindrical coordinate system taking the symmetry of the nanowire model into account. We can reduce the number of points in the PES calculation along axial and angular directions. The parameters of the hydrogen coordinate are taken as shown in fig. 1, and their ranges are given as follows,

$$0 \leq \rho \leq R_D, \quad (1)$$

$$0 \leq \theta \leq \frac{\pi}{5}, \quad (2)$$

$$0 \leq z \leq 1.23 \text{ \AA}. \quad (3)$$

Here a new radial constant  $R_D$  is taken as  $R_D = R + 2.50 = 4.97 \text{ \AA}$ . Once energies are calculated only for this region, the PES for the required region can be derived. The adsorption energy ( $\Delta E$ ) is defined as follows,

$$\Delta E = E_{\text{NW+H}} - E_{\text{NW}} - E_{\text{H}_2}/2, \quad (4)$$

where  $E_X$  means the total energy of the system X. The definition of  $\Delta E$  is calculated for the hydrogen molecule instead of the hydrogen atom for comparison with other works. At the dissociation limit, the adsorption energy in this system is 2.24 eV. In the calculation of the PES, the deformation of the nanowire is not taken into account, since the motivation of this work is the study of the dynamics of hydrogen and deuterium atoms on the nanowire. The aluminum atom is much heavier than the hydrogen atom. Hence, the motion of the aluminum atom is negligible during the motion of the hydrogen atom. The calculation mesh size of the radial direction is taken as  $0.1 \text{ \AA}$ , that of the angular direction is  $\pi/50$ , and that of the axial direction is  $0.123 \text{ \AA}$ .

For the calculation of the wave function of hydrogen and deuterium atoms, we solve the three dimensional Schrödinger equation. The PES calculated in this work is used as the potential term of this calculation. Periodic boundary conditions are imposed on axial and angular directions. For the radial direction, the boundary condition is given as,

$$\Psi_{\text{H}}(R_D, \theta, z) = 0. \quad (5)$$

We choose  $R_D$ , instead of the infinity, as the boundary condition of the radial direction for simplicity. This choice of the boundary condition is sufficient for

this work. The length of this unit cell in the axial direction is  $4D$ , which is half as long as that of the super cell used in electronic structure calculation. The wave function is expanded by plane wave and Bessel function basis sets as follows,

$$\begin{aligned}\Psi_{\text{H}}(\rho, \theta, z) &= \sum_{l,m,n} C_{lmn} \psi_{lmn}(\rho, \theta, z), \quad (6) \\ \psi_{lmn}(\rho, \theta, z) &= \frac{\sqrt{2}}{R_D J_{m+1}(x_{mn})} J_m \left( x_{mn} \frac{\rho}{R_D} \right) \\ &\times \frac{1}{\sqrt{2\pi}} \exp(im\theta) \\ &\times \frac{1}{\sqrt{4D}} \exp\left(il2\pi \frac{z}{4D}\right), \quad (7)\end{aligned}$$

where  $J_m$  means the first kind Bessel function of order  $m$  and  $x_{mn}$  is the  $n$ th zero point of the Bessel function of order  $m$ . The expansion coefficient,  $C_{lmn}$ , is derived from the diagonalization of the Hamiltonian. Considering the symmetry of this model,

$$\Psi_{\text{H}}(\rho, \theta + \pi/5, z + 2D) = \Psi_{\text{H}}(\rho, \theta, z). \quad (8)$$

Accordingly, wave vectors of axis and radial directions can be given as,

$$m \frac{\pi}{5} + l2\pi \frac{2D}{4D} = 2N\pi \quad (l, m, N = 0, \pm 1, \pm 2, \dots). \quad (9)$$

This equation is simplified to

$$m' + l = 2N \quad (m' = 0, \pm 1, \pm 2, \dots), \quad (10)$$

$$m = 5m'. \quad (11)$$

In this calculation, the ranges of the parameters  $(n, m', l)$  are applied as follows,

$$n = 1, \dots, 10, \quad (12)$$

$$m' = 0, \pm 1, \pm 2, \pm 3, \pm 4, \quad (13)$$

$$l = 0, \pm 1, \dots, \pm 40. \quad (14)$$

Thus the number of the basis functions is 3730. In addition,  $\psi_{nml}(\rho, \theta, z)$  is an orthogonal system,

$$\langle \psi_{nml} | \psi_{n'm'l'} \rangle = \delta_{nn'} \delta_{mm'} \delta_{ll'}. \quad (15)$$

The term of the kinetic energy can be calculated analytically,

$$\langle \psi_{nml} | K | \psi_{nml} \rangle = \frac{\hbar^2}{2m_X} \left[ \left( \frac{x_{nm}}{R_D} \right)^2 + \left( l \frac{2\pi}{4D} \right)^2 \right], \quad (16)$$

where  $m_X$  means the mass of a hydrogen atom or a deuterium atom. The integration of the potential energy term is carried out using Gauss-Legendre method.

We analyze electronic states and properties using quantum energy density, which is proposed by one of the authors [18]. One of the quantity of the quantum energy density, the electronic kinetic energy density  $n_T(\vec{r})$ , is defined as

$$n_T(\vec{r}) = \frac{1}{2} \sum_i \nu_i \left\{ \left[ -\frac{\hbar^2}{2m_e} \Delta \psi_i^*(\vec{r}) \right] \psi_i(\vec{r}) + \psi_i^*(\vec{r}) \left[ -\frac{\hbar^2}{2m_e} \Delta \psi_i(\vec{r}) \right] \right\}, \quad (17)$$

where  $m_e$  is the mass of the electron,  $\psi_i(\vec{r})$  is the  $i$ th natural orbital, and  $\nu_i$  is the occupation number of  $\psi_i(\vec{r})$ . The electronic kinetic energy of the system is obtained by integration of kinetic energy density over the whole space. In classical mechanics, only positive kinetic energy is allowed, and however negative kinetic energy appears in quantum mechanics. This means that electrons can exist also in regions with the negative kinetic energy density with quantum effects. The surface of zero kinetic energy density can be interpreted as the boundary of a molecule.

In the calculation of the kinetic energy density, we use two program codes for each boundary condition, respectively. The electronic state is calculated by fhi98md program package [22] for the periodic system and Gaussian 03 program package [23] for the molecular system. The kinetic energy density is calculated based on these electronic states by Periodic Regional DFT (PRDFT) program package [24] for the periodic system and Molecular Regional DFT (MRDFT) program package [25] for the molecular system. The calculation of the nanowire model uses, of course, the periodic boundary condition. On the other hand, the calculation of the molecular system is also performed for the cluster system,  $\text{Al}_{13}$ , which has the same structure of a part of the nanowire. This calculation is for a comparison with the nanowire.

### 3. Result and Discussion

#### 3.1. Electronic structure of aluminum nanowire model

Before the discussion of the migration of the hydrogen atom, we discuss the electronic structure and charge transfer of the nanowire model without and with the adsorbed hydrogen. In our previous paper, we have shown that electron density is higher for aluminum atoms on the axis compared to those of rings [15].

In fig. 2, we show total DOS (TDOS) and partial DOS (PDOS) of aluminum atoms of pentagonal rings and those on the axis for the aluminum nanowire model without the adsorbed hydrogen. The Fermi level is taken to be 0.0 eV shown as vertical dotted lines in figures. In both TDOS and PDOS, some peak structures are seen, which may be characteristic for one dimensional metallic nanowire. Comparing figs. 2(b) and (c), contributions from  $p$  and  $d$  orbitals are

large for aluminum atoms on the axis in the low-energy region. This is because electron density is distributed along the axial direction as shown in our previous paper [15].

In fig. 3, we show TDOS of the nanowire model with the adsorbed hydrogen and PDOS of the aluminum atom adsorbed by the hydrogen atom, those on the axis, and those of the hydrogen atom. The Fermi level is taken to be 0.0 eV shown as vertical dotted lines in figures. Compared with fig. 2, the shape of the peak near the Fermi level in TDOS is modified significantly after the hydrogen adsorption. This modification originates in the aluminum atom adsorbed by the hydrogen atom as can be seen in the figure of its PDOS. The changes of TDOS and PDOS in the low energy region are not significant. PDOS of the hydrogen atom is distributed over wide range of the energy.

In order to study the electronic structure of these models, we study also the amount of charge transfer. We calculate the number of valence electrons for aluminum atoms on the ring and on the axis for the aluminum nanowire model without the adsorbed hydrogen atom. To do so, we use the PDOS in this work. These results are shown in table 1. Al(ring) means atoms on the pentagonal rings and Al(axis) means atoms on the axis. As seen in this table, the charge is transferred from pentagonal rings to the axis. In particular, electrons in  $p$  and  $d$  orbitals increase, while there is little difference for those of  $s$  orbital.

Next, we consider the charge transfer caused by the hydrogen adsorption. In this calculation, we consider that the hydrogen atom is adsorbed on the top site of the aluminum nanowire, which is the most stable site as shown in the next subsection. The results of the charge transfer is shown in table 2. In this table, Al(ring)<sub>1</sub> represents the aluminum atom on which the hydrogen is adsorbed, Al(ring)<sub>2</sub> represents aluminum atoms on pentagonal rings except for Al(ring)<sub>1</sub>, and Al(axis) represents those on the axis. Since the distances from the hydrogen atom to the aluminum atoms are different for each atom in Al(ring)<sub>2</sub> and Al(axis), only the range of values is dictated in table 2. After the hydrogen adsorption, the number density of electrons on Al(ring)<sub>1</sub> increases as seen by comparing with table 1. This increase is compensated by the decrease of that on the hydrogen atom. Significant changes for Al atoms on the axis are not seen. Focusing on each orbital in Al(ring)<sub>1</sub>, the number densities of electrons on  $p$  and  $d$  orbital increase and that on  $s$  orbital decreases. In other words, electrons are transferred to orbitals which have directionality.

In the following, we discuss the migration of the adsorbed hydrogen atom. The hydrogen atom is slightly charged, and hence, we can roughly estimate how large electric field drives the hydrogen atom, once we know the potential barrier. However, this is not so straightforward, since the potential barrier will be modified by electric fields. We do not discuss further this point.

### 3.2. Potential energy surface and diffusion path of a hydrogen atom

Results of PES calculations are shown in fig. 4 for  $z = 0D$ ,  $4D/5$ , and  $1D$  surfaces, which are characteristic ones. The position of the most stable point is  $(\rho, \theta, z) = (4.07 \text{ \AA}, 0, 0D)$  and its adsorption energy is calculated as 0.12 eV. This means that the depth of this PES in the radial direction is large

and the hydrogen desorption is not easy. As seen in fig. 4, the gradient of the PES along the radial direction is much larger than that along the angular and axial directions. This means that we can parametrize adsorption points by  $\theta$  and  $z$ . The difference of the adsorption energy from the most stable point  $(\theta, z) = (0, 0D)$  is shown as a function of  $\theta$  and  $z$  in fig. 5(a). The value of  $\rho$  is taken so that the adsorption energy is minimum, which is shown in fig. 5(b). It can be seen that the range of  $\rho$  is almost limited within 1 Å. The adsorption energy has a strong correlation with the value of  $\rho$ . The most stable point on  $z = 1D$  surface is given for  $(\rho, \theta, z) = (3.47 \text{ Å}, \pi/10, 1D)$ . The most stable point as a function of  $z$  is shifted from  $\theta = 0$  to  $\theta = \pi/10$  around  $z = 4D/5$ . This is due to the difference of the angle between pentagonal rings.

We consider two paths of the hydrogen diffusion, axial and angular directions, as shown in fig. 6. Path A is the move toward the axial direction and path B shows that toward the angular direction. For path A, we consider the shift of  $\theta$  together, since the most stable point for  $z = 1D$  is given by  $\theta = \pi/10$ . The energy curves along path A and B are shown as a function of  $z$  and  $\theta$ , respectively, which are normalized by  $D$  and  $\theta_0 = \pi/5$ . In the case of path A, the activation energy is the highest at  $z = 4D/5$  whose energy is 0.19 eV. Then the hydrogen atom is in a metastable state at  $(\rho, \theta, z) = (3.47 \text{ Å}, \pi/10, 1D)$ . In this position, the distances from the hydrogen atom to the two nearest aluminum atoms on the different pentagonal rings are the same. On the other hands, the peak of energy of path B is given at  $\theta = 4\theta_0/5$ , and the activation energy is 0.57 eV. As in the case of path A, the hydrogen atom is in a metastable state at  $(\rho, \theta, z) = (3.07 \text{ Å}, \pi/5, 0D)$ , and the distances from the hydrogen atom to the two nearest aluminum atoms on the same pentagonal ring are the same. From these results, the hydrogen atom can move to the axial direction more easily. The distance from one aluminum atom on a pentagonal ring to another atom on the same pentagonal ring is equal to that on the next different pentagonal rings (2.90 Å). However the activation energies for the hydrogen diffusion along the path A and B are quite different. One difference is the distance from the initial position. To compare the distances, we consider simply the cylinder of the radius 4.07 Å, the distance from one adsorption point to another point on the same pentagonal ring is 5.11 Å. On the other hands, the distance from one adsorption point to the next different pentagonal rings is 3.58 Å. Thus the length of path A is shorter than that of the other.

The difference between two paths can also be seen in the viewpoint of the kinetic energy density. The kinetic energy density calculation is carried out for the aluminum nanowire without the hydrogen atom. Figures 7(a) and (b) show the value of  $\rho$  and the potential energy, where the kinetic energy density is zero, as a function of  $\theta$  and  $z$ . Compared to fig. 5, the surface of the zero kinetic energy density and that of the minimum potential energy surface have the pattern similar to each other. In both isosurfaces of  $\rho$ , there is a deeper dent for the radial direction between aluminum atoms on the same pentagonal ring than that on different pentagonal rings. The values of the adsorption energy are almost the same as those for PES, since  $\rho$  is also almost the same. The zero kinetic energy density surface is originally proposed as a surface of

a molecule [18]. This implies that the minimum potential energy surface is quite similar to the nanowire surface. Hence the hydrogen diffusion path may be roughly identified with the shortest path on this surface. This character of the zero kinetic energy density surface can also be seen in  $\text{Al}_{13}$  cluster model which has two pentagonal rings and three Al atoms on the axis. This surface is obtained by a molecular system calculation [23, 25]. Hence this character is due to two pentagonal rings structure and not peculiar to a nanowire model.

### 3.3. Wave function of hydrogen and deuterium atoms

In fig. 8, we show the probability densities of the hydrogen atom from the ground state to the ninth excited state. The isosurfaces are depicted for the value,  $0.01[1/\text{\AA}^3]$ , and  $\epsilon$  is the energy eigenvalue. In the ground state, the probability density is localized around the top site of an aluminum atom. This position corresponds to that of the minimum of the PES. The energy eigenvalue of the ground state is 0.34 eV, so that the zero-point vibrational energy is estimated as 0.22 eV. Patterns of probability densities in excited states are divided into two kinds. In one of patterns, the probability densities are distributed around the top site of an aluminum atom ( $z \sim 0$  and  $\theta \sim 0$ ). In the other pattern, the probability densities are seen around the intermediate point of the axial migration path, i.e. between aluminum pentagonal rings, ( $z \sim D$  and  $\theta \sim 10/\pi$ ). Note that the migration path to the axial direction is accompanied by the angular rotational shift of  $\pi/5$ . The latter group consists of, the sixth, seventh, and eighth excited states. The density is high enough at the intermediate point of the migration path of the axial direction, where the potential energy surface has high value as seen in fig. 6. Their energy eigenvalues are 0.42 eV (sixth) and 0.43 eV (seventh and eighth), respectively. (The seventh and the eighth excited states are not degenerate, though they can be seen so within this accuracy.) The energy difference between the sixth excited state and the ground state is 0.08 eV. This energy difference is much smaller than the activation energy of the PES calculation, 0.19 eV. As a result, the diffusion of the hydrogen atom to the axial direction through excited states in the quantum picture requires smaller energy compared to the estimate by the classical picture. In addition, the diffusion to the angular direction is seen to be not favored even in the quantum picture.

In fig. 9, we also show the probability densities of a deuterium atom. The value of isosurfaces is the same as fig. 8. The energy eigenvalue of the ground state is 0.31 eV, which is less than that for the hydrogen atom by 0.03 eV. The difference originates in the difference of the mass between the hydrogen and deuterium atoms and results in the decrease of the zero-point vibrational energy. In the ground state, the distribution of the probability density is almost the same as in the case of the hydrogen atom, while the order of the distribution pattern is replaced in some excited states. Specifically, the pattern of sixth excited state in the hydrogen atom appears in the eighth excited state. These states are the lowest among states that the probability densities are seen between aluminum pentagonal rings. The energy difference between the ground state and this



excited state is 0.09 eV. The discrepancy from that of the hydrogen atom is not so large. Therefore, deuterium atoms also travel to the axial direction through excited states.

#### 4. Summary

We have studied the behavior of a hydrogen atom on aluminum nanowire based on density functional theory. First we have calculated the potential energy surface. The most stable position of the adsorbed hydrogen atom is the top site of an aluminum atom, and the adsorption energy is 0.12 eV. The activation energy of the hydrogen diffusion to the axis direction is 0.19 eV, while that to the angular direction is 0.57 eV. Thus the hydrogen can travel to the axial direction more easily. We have also studied quantum effects of the adsorbed hydrogen and deuterium atoms. The probability density of the hydrogen atom in the ground state is localized at the top site of an aluminum atom. In some excited state, the probability density is distributed between pentagonal rings. The energy difference from the ground state is 0.08 eV, which is much smaller than the activation energy in the PES calculation. On the other hand, in the case of the deuterium atom, the energy eigenvalues are lowered slightly. The energy difference between the ground state and the excited state distributed between pentagonal rings increases slightly and is calculated as 0.09 eV. These results imply that the diffusion of the hydrogen and deuterium atoms to the axial direction through excited states in the quantum picture requires smaller energy compared to the estimate by the classical picture.

#### Acknowledgments

This work was partially supported by the Ministry of Education, Science, Sports and Culture, Grant-in-Aid for Scientific Research on Priority Areas, 20035006 and 20038029. The computations were partially performed using Research Center for Computational Science, Okazaki, Japan.

#### References

- [1] Y. Kondo and K. Takayanagi, *Science* 289 (2000) 606.
- [2] V. Rodrigues, T. Fuhrer, D. Ugarte, *Phys. Rev. Lett.* 85 (2000) 4124.
- [3] A. Nakamura, M. Brandbyge, L. B. Hansen, K. W. Jacobsen, *Phys. Rev. Lett.* 82 (1999) 1538.
- [4] O. Gülseren, F. Ercolessi, E. Tosatti, *Phys. Rev. Lett.* 80 (1998) 3775.
- [5] T. Makita, K. Doi, K. Nakamura, A. Tachibana, *J. Chem. Phys.* 119 (2003) 538.

- [6] M. Suzuki, K. Nagai, S. Kinoshita, K. Nakajima, K. Kimura, T. Okano, K. Sasakawa, *Appl. Phys. Lett.* 89 (2006) 133103.
- [7] M. Saka and R. Ueda, *J. Mater. Res.* 20 (2005) 10.
- [8] Y. Kawakami, T. Kikura, K. Doi, K. Nakamura, and A. Tachibana, *Mater. Sci. Forum.*, 426-432 (2003) 2399.
- [9] A. Goldberg, I. Yarovsky, *Phys. Rev. B* 75 (2007) 195403.
- [10] M. F. Luo, G.R. Hu, *Surf. Sci.* 603 (2009) 1081.
- [11] H. Nakano, H. Ohta, A. Yokoe, K. Doi, A. Tachibana, *J. Power Sources* 163 (2006) 125.
- [12] R. M. Nieminen, M. J. Pusuka, *Physica* 127B (1984) 417.
- [13] M. J. Pusuka, R. M. Nieminen, *Surf. Sci.* 157 (1985) 413.
- [14] P. Sen, O. Gülseren, T. Yildirim, I. P. Batra, and S. Ciraci, *Phys. Rev. B* 65 (2002) 235433.
- [15] A. Fukushima, K. Doi, M. Senami, A. Tachibana, *J. Power Source* 184 (2008) 60.
- [16] G. Källén, G. Wahnström, *Phys. Rev. B* 65 (2001) 033406.
- [17] K. Nobuhara, H. Nakanishi, H. Kasai, A. Okiji, *Surf. Sci.* 493 (2001) 271.
- [18] A. Tachibana, *Int. J. Quantum Chem. Symp.* 21 (1987) 181; A. Tachibana, R.G. Parr, *Int. J. Quantum Chem.* 41 (1992) 527; A. Tachibana, *Int. J. Quantum Chem.* 57 (1996) 423; A. Tachibana, *Theor. Chem. Acc.* 102 (1999) 188; A. Tachibana, *J. Chem. Phys.* 115 (2001) 3497; A. Tachibana, *Stress Induced Phenomena in Metallization*, American Institute of Physics, New York, (2002), p. 105; A. Tachibana, in: E. Brändas, E. Kryachko (Eds.), *Fundamental Perspectives in Quantum Chemistry: A Tribute to the Memory of Per-Olov Löwdin*, vol. II, Kluwer Academic, Dordrecht, (2003), p. 211; A. Tachibana, *J. Mol. Model* 11 (2005) 301; A. Tachibana, *J. Mol. Struct. (THEOCHEM)* 943 (2010) 138.
- [19] G. Kresse and J. Hafner, *Phys. Rev. B* 47 (1993) 558; G. Kresse and J. Hafner, *Comput. Mater. Sci.* 6 (1996) 15; G. Kresse and J. Furthmüller, *Phys. Rev. B* 54 (1996) 11169.
- [20] G. Kresse and D. Joubert, *Phys. Rev. B* 59 (1999) 1758.
- [21] J. P. Perdew, K. Burke, M. Ernzerhof, *Phys. Rev. Lett.* 77 (1996) 3865.
- [22] M. Bockstedte, A. Kley, J. Neugebauer, M. Scheffler, *Comp. Phys. Comm.* 107 (1997) 187.

- [23] M. J. Frisch *et al.*, Gaussian 03, Revision B.05, Gaussian, Inc., Pittsburgh PA (2003).
- [24] Periodic Regional DFT Program Package, ver. 3, Tachibana Lab., Kyoto University, Kyoto (2008); For example see, K. Doi, K. Nakamura and A. Tachibana, The proceedings of 2006 International Workshop on Nano CMOS (2006) 209.
- [25] Molecular Regional DFT Program Package, ver. 3, Tachibana Lab., Kyoto University, Kyoto (2008); For example see, K. Doi, K. Nakamura and A. Tachibana, The proceedings of 2006 International Workshop on Nano CMOS (2006) 209.

Table 1: Number of valence electrons calculated from PDOS. Al(ring) and Al(axis) mean an aluminum atom on a pentagonal ring and on the axis, respectively.

Atom	s-orbital	p-orbital	d-orbital	total
Al(ring)	1.245	1.285	0.289	2.820
Al(axis)	1.228	2.014	0.659	3.902

Table 2: Number of valence electrons calculated from PDOS. Al(ring)<sub>1</sub> is the aluminum atom on which the hydrogen is adsorbed and Al(ring)<sub>2</sub> is aluminum atoms on pentagonal rings except for Al(ring)<sub>1</sub>. For Al(ring)<sub>2</sub> and Al(axis), only the range of values is given.

Atom	s-orbital	p-orbital	d-orbital	total
Al(ring) <sub>1</sub>	1.156	1.616	0.409	3.181
Al(ring) <sub>2</sub>	1.241-1.254	1.260-1.301	0.281-0.291	2.813-2.834
Al(axis)	1.225-1.230	1.987-2.030	0.650-0.678	3.895-3.905
H	0.620	0.010	0.001	0.630

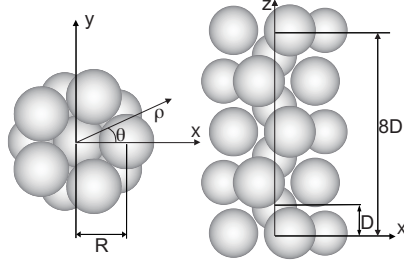


Fig. 1: Calculation model of aluminum nanowire. This model has pentagonal rings whose angles are different by  $\pi/5$  from each other.  $R$  is the radius of the pentagonal ring,  $D$  is the half-distance between aluminum atoms on the axis, and  $8D$  is the unit cell length.  $\rho$ ,  $\theta$ , and  $z$  are used for a cylindrical coordinate system in PES calculations.

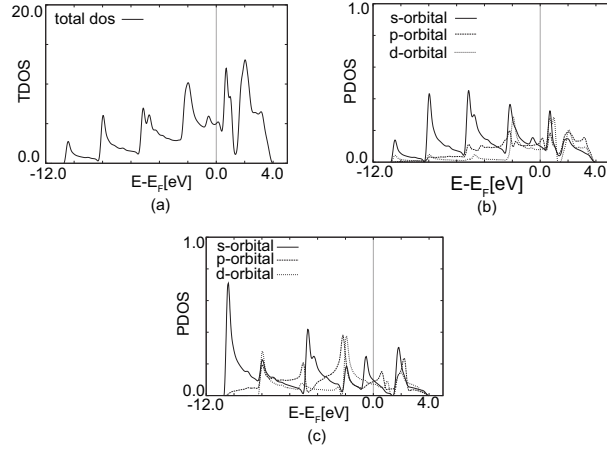


Fig. 2: TDOS and PDOS of the nanowire model, (a) TDOS of this model, (b) PDOS of atoms on the pentagonal ring, and (c) PDOS of atoms on the axis, respectively. The Fermi level is taken to be 0.0 eV shown as vertical dotted lines.

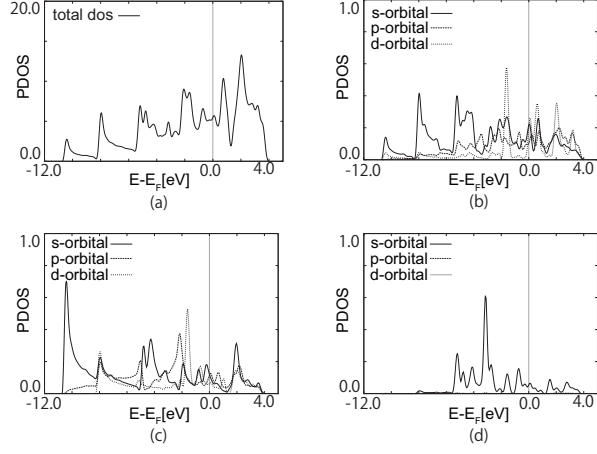


Fig. 3: TDOS and PDOS of the nanowire model, (a) TDOS of this model, (b) PDOS of the aluminum atom on which the hydrogen is adsorbed, (c) PDOS of aluminum atoms on the axis, and (d) PDOS of the hydrogen atom, respectively. The Fermi level is taken to be 0.0 eV shown as vertical dotted lines.

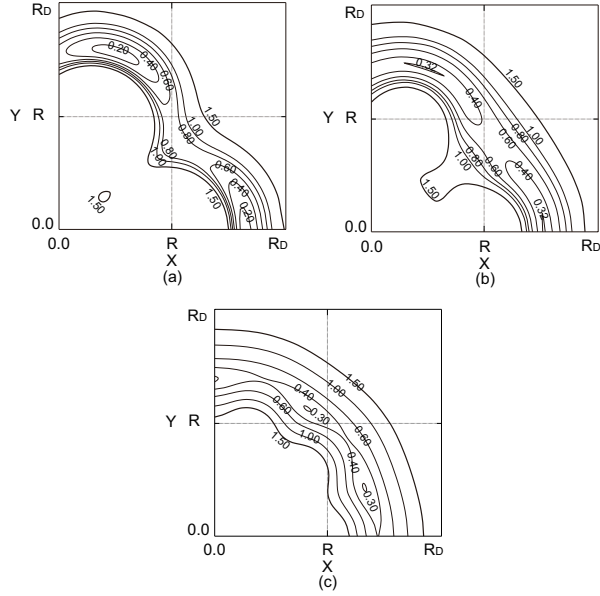


Fig. 4: Potential energy surface of the hydrogen atom adsorption. (a)  $z = 0D$  surface, (b)  $z = 4D/5$  surface, and (c)  $z = 1D$  surface. The unit of the energy is eV.

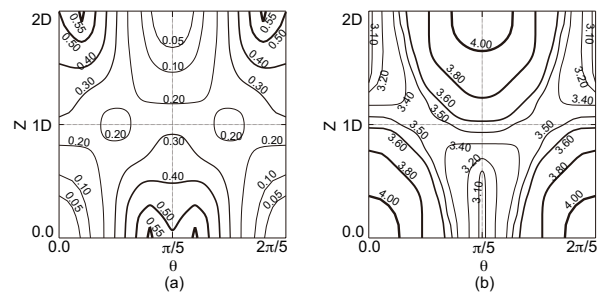


Fig. 5: (a) The difference of the potential energy surface as a function of  $\theta$  and  $z$ . The unit of the energy is eV. The value of  $\rho$  is taken as that in figure (b). (b) The value of  $\rho$  so that the adsorption energy is minimum as a function of  $\theta$  and  $z$ . The unit of  $\rho$  is  $\text{\AA}$

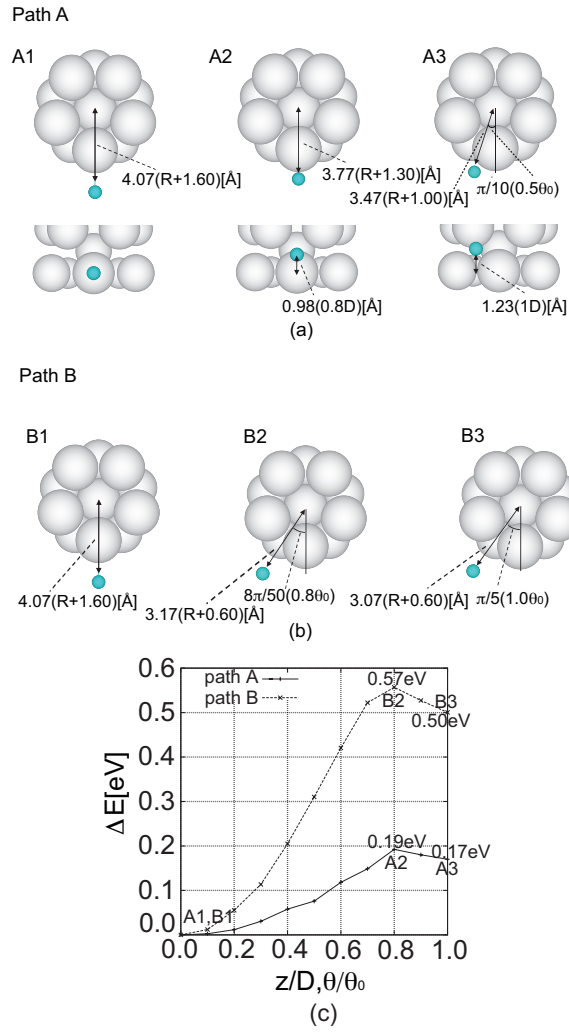


Fig. 6: Paths for the move of a hydrogen atom and the energy along these paths. (a) three typical points in path A, (b) three typical points in path B, and (c) the energy curves of paths A and B as a function of  $z$  and  $\theta$  ( $\theta_0 = \pi/5$ ), respectively. A(1,2,3) and B(1,2,3) correspond to points in figures (a) and (b).



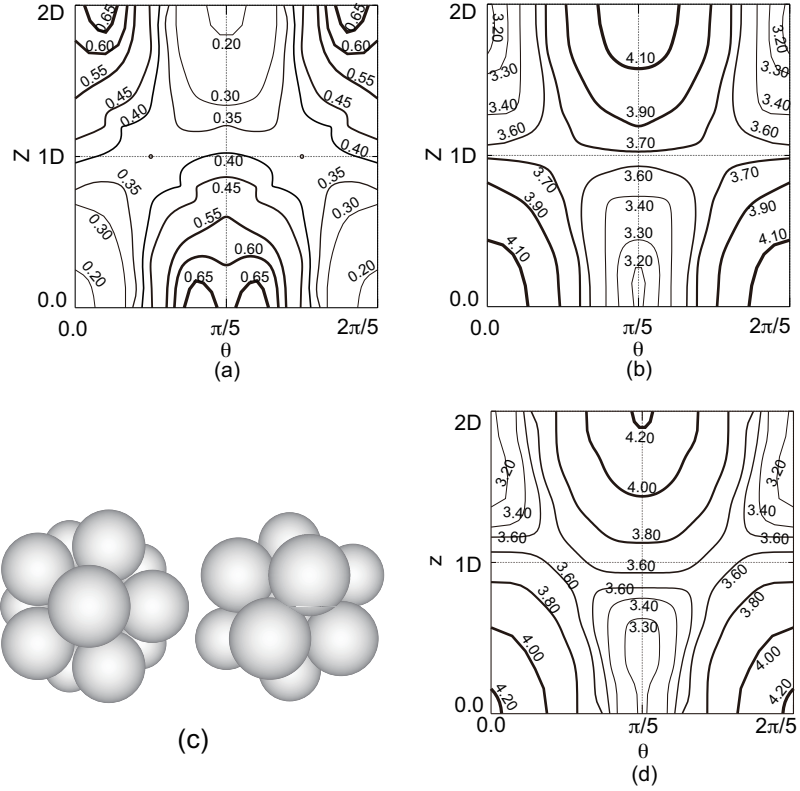


Fig. 7: (a) The value of  $\rho$  where the kinetic energy density is zero, as a function of  $\theta$  and  $z$ . The unit of  $\rho$  is  $\text{\AA}$ . (b) The potential energy as a function of  $\theta$  and  $z$ . The unit of energy is eV. The value of  $\rho$  is taken as that in figure (a). (c) The calculation model of  $\text{Al}_{13}$  cluster. The radial parameter ( $R$ ) and the half-distance between aluminum atoms on the axis ( $D$ ) are the same as those of the nanowire model. (d) The value of  $\rho$  where the kinetic energy density is zero, as a function of  $\theta$  and  $z$  for the  $\text{Al}_{13}$  cluster model.

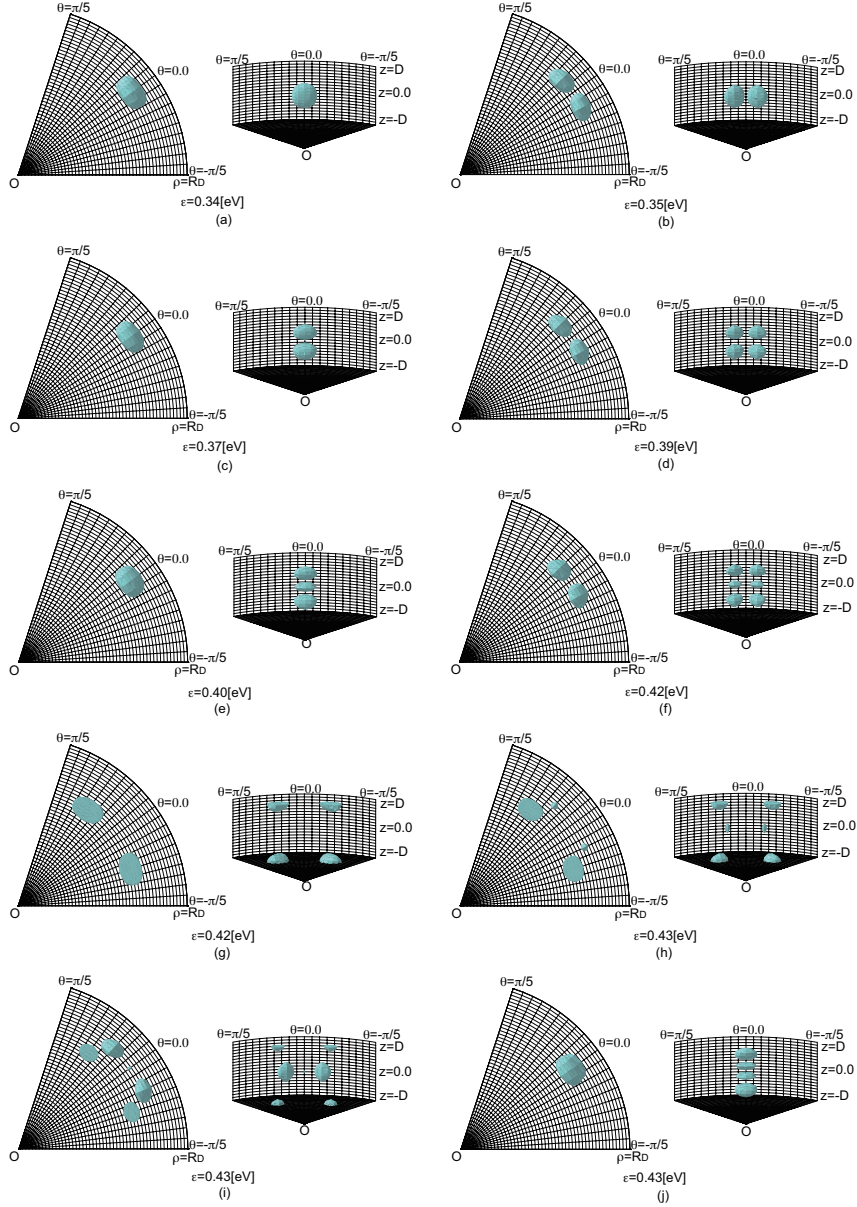


Fig. 8: The distribution of the probability densities of the hydrogen atom from the ground state to the ninth excited state. The isosurfaces are depicted for the value,  $0.01[1/\text{\AA}^3]$ , and  $\epsilon$  is the energy eigenvalue.

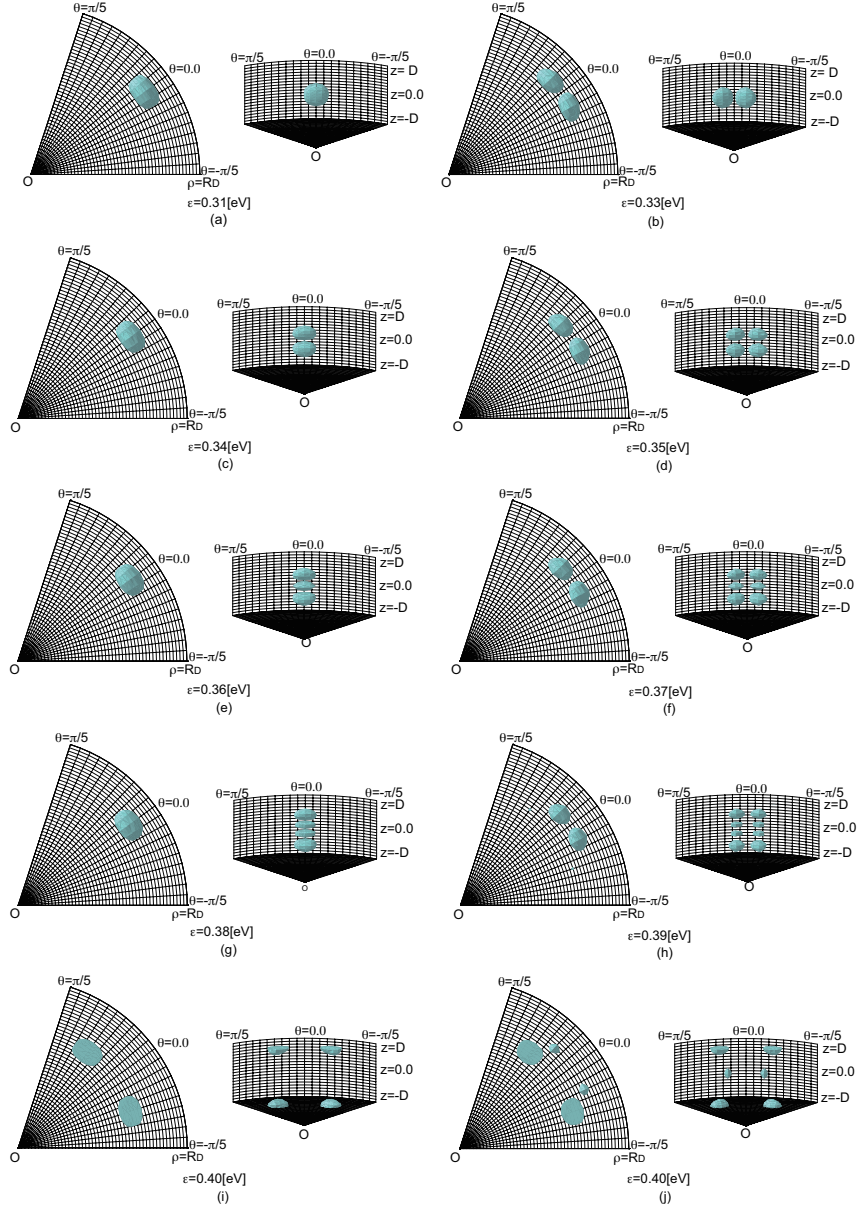


Fig. 9: The distribution of the probability densities of the deuterium atom from the ground state to the ninth excited state. The isosurfaces are depicted for the value,  $0.01[1/\text{\AA}^3]$ , and  $\epsilon$  is the energy eigenvalue.